Supplementary Materials for

# Optical nonlocal meta-grating computing spatiotemporal differentiation

Junyi Huang[1,#], Dong Zhao[2,#], Jixuan Shi[2,3,#], Hengyi Wang[2], Hongliang Zhang[1], Fangwen Sun[2], Qiwen Zhan[5], Kun Huang[2,*], Zhichao Ruan[1,**]

[1] School of Physics, State Key Laboratory of Extreme Photonics and Instrumentation, and Zhejiang Province Key Laboratory of Quantum Technology and Device, Zhejiang University, Hangzhou 310027, China
[2] Department of Optics and Optical Engineering, University of Science and Technology of China, Hefei 230026, China
[3] Department of Physics, Tsinghua University, Beijing 10010, China
[4] College of Optical Science and Engineering, Zhejiang University, Hangzhou 310027, China
[5] School of Optical-Electrical and Computer Engineering, University of Shanghai for Science and Technology, Shanghai 200093, China

# These authors contributed equally to this work
* huangk17@ustc.edu.cn
** zhichao@zju.edu.cn

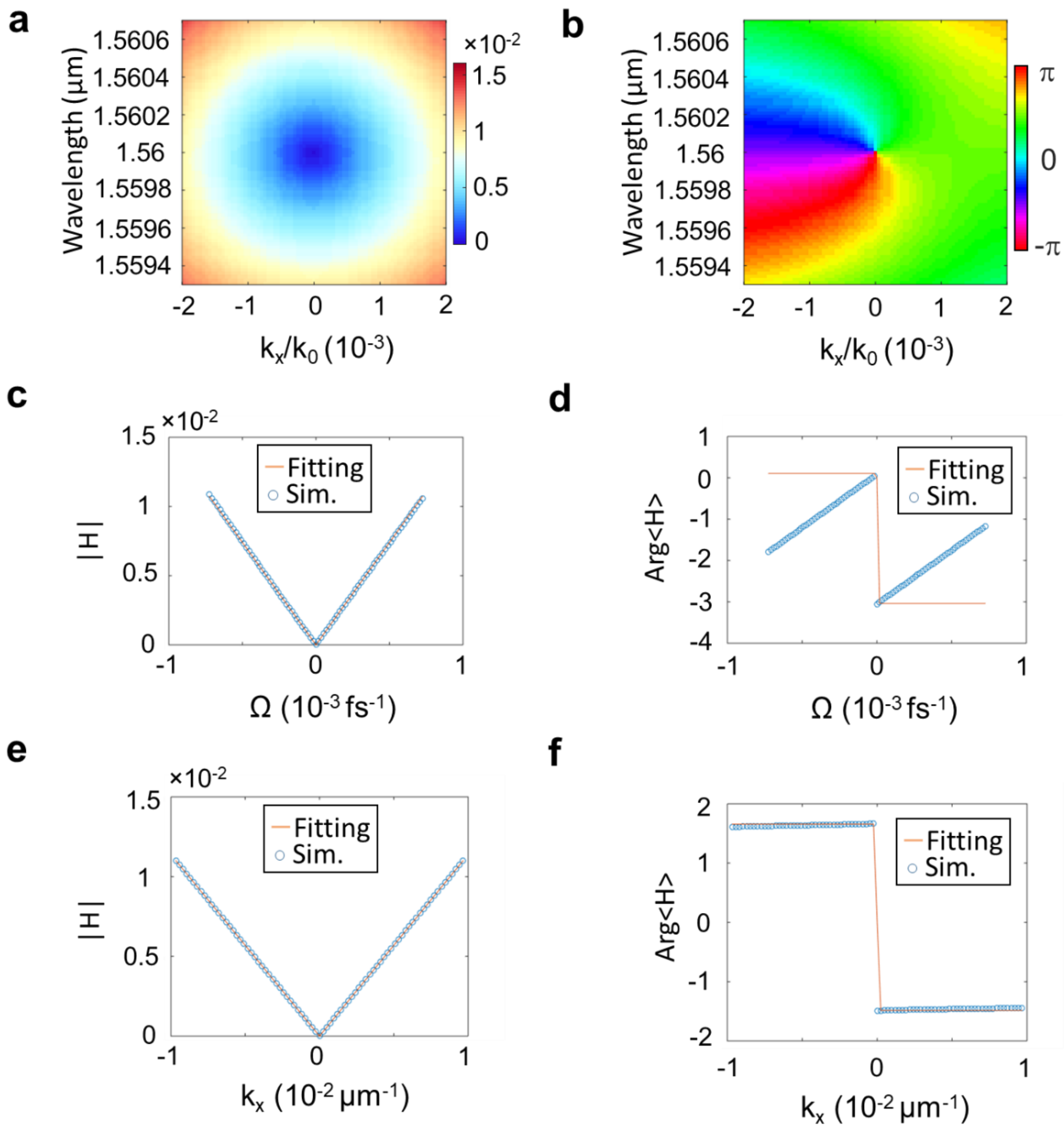


**Extended Data Figure 1. Simulated properties of the proposed spatiotemporal differentiators**. **(a-b)** Simulated amplitude **(a)** and phase **(b)** of the transmission function H. **(c-d)** Line-scanning amplitude **(c)** and phase **(d)** of transmission function H with a variable of the temporal frequency $\Omega$ at $k_x$=0. The linear fitting (solid lines) is employed to predict the differentiation strength $C_t$. (e-f) Line-scanning amplitude **(e)** and phase **(f)** of transmission function H with a variable of the spatial frequency $k_x$ at $\Omega$=0. The linear fitting (solid lines) is employed to predict the differentiation strength $C_x$.

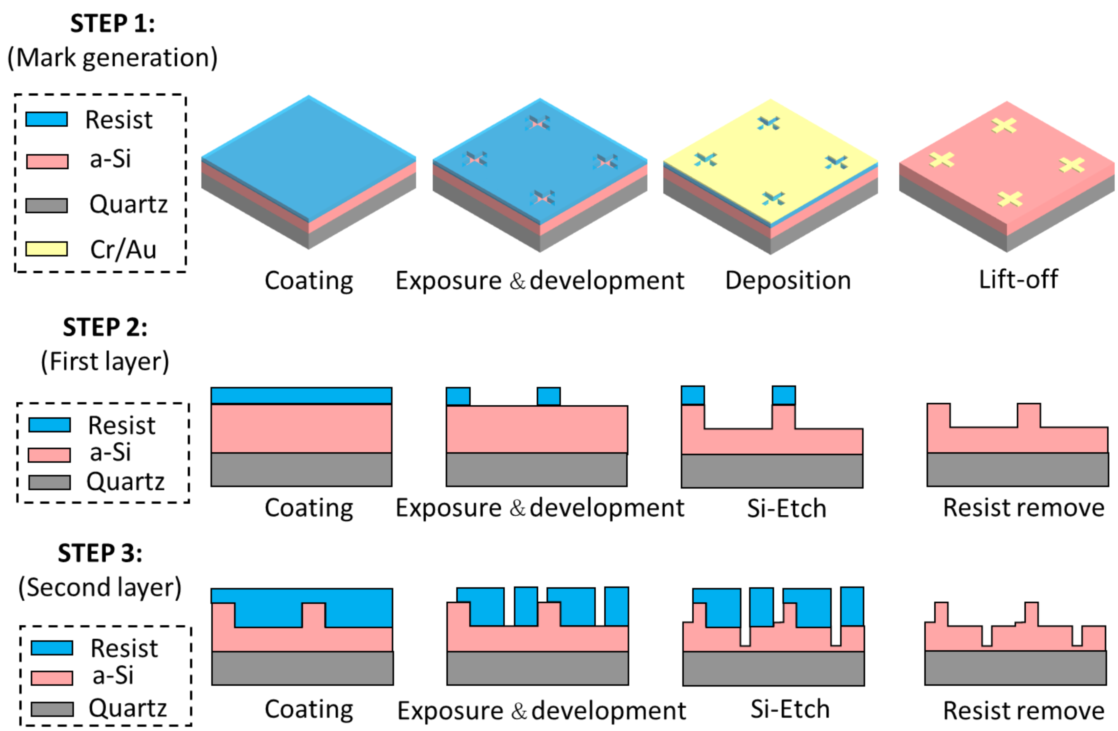


**Extended Data Figure 2. Fabrication sketch for our meta-grating-based spatiotemporal differentiators**. The fabrication includes three processes: mark generation, first-layer patterning, and second-layer patterning. The details of fabrication is provided in the Method of main text.

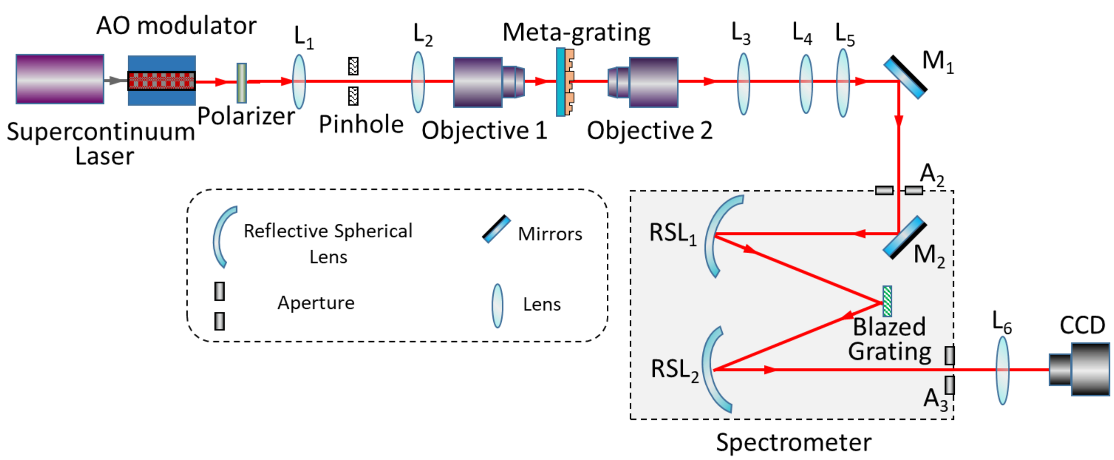


**Extended Data Figure 3. Experimental setup for measuring optical transmission $|H|^2$ of our meta-grating in a configuration of optical spectroscopy**. A supercontinuum laser (SuperK Fianium FIU-15) with a broadband operating spectrum from 410 nm to 2400 nm is filtered by an acoustic-optic (AO) modulator, yielding a quasi-monochromic light source. To obtain the required polarization, the light passes through a linear polarizer before being expanded by a telescope system (composed of two lenses $L_1$ and $L_2$) and filtered spatially by a pinhole. To realize a large range of spatial frequency, an objective 1 is used to focus the light on our fabricated meta-grating sample.

After the transmitted light is collected by another objective lens 2, a couple of lenses ($L_3$, $L_4$ and $L_5$) are used to project the spatial frequency of our meta-grating onto the entrance $A_2$ of an optical spectroscopy (composed of the key components: a blazed grating and two reflective spherical mirrors). In this spectroscopy, the conjugate port of the $A_2$ is the exit $A_3$, where the information of both spatial and temporal frequencies are located. To capture them, an additional imaging lens $L_6$ is used to project the frequency information onto a CCD camera.

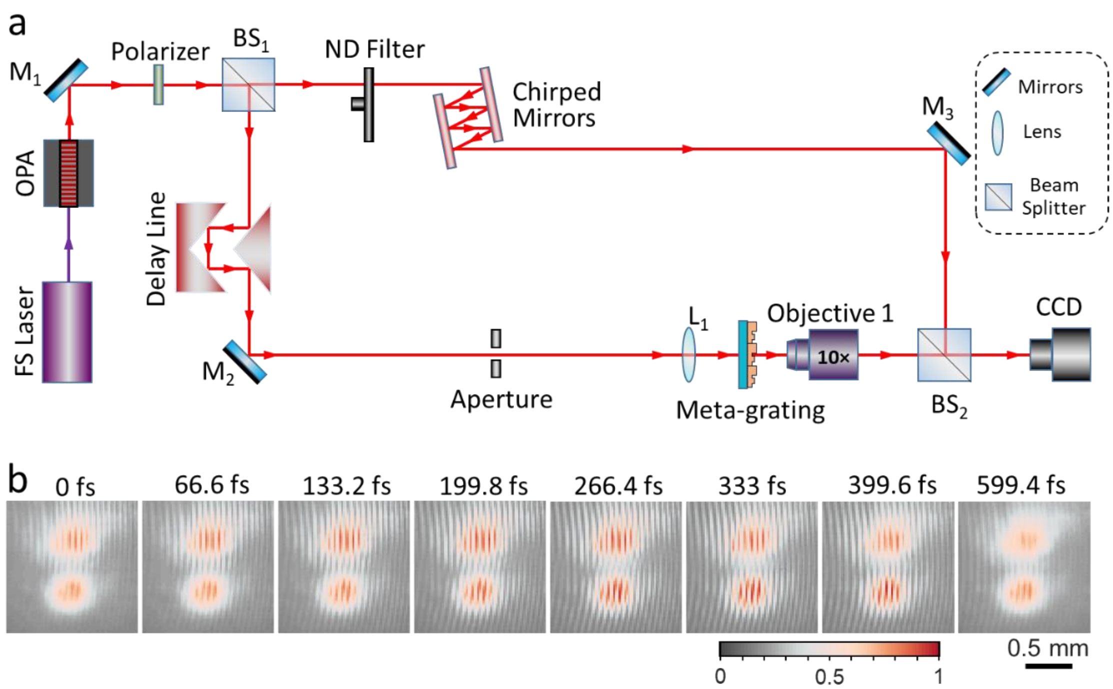


**Extended Data Figure 4. Experimental characterization of our meta-grating-based spatiotemporal differentiator**. **(a)** Optical setup for measuring the spatiotemporal properties of the transmitted pulse through our meta-grating in a Mach-Zender interferometer. In this interferometer, the pulse in the reference arm is suppressed by two chirped mirrors, while the delay line composed of two complementary prisms is located in the signal beam to tune optical path for generation of the interference patterns, which are recorded by a CCD camera after projected and magnified by an objective 1. **(b)** Recorded interference patterns with a time interval of 33.3 fs. The dislocation between the upper and lower interference fringes happens, implying the creation of the spatiotemporal phase singularity.

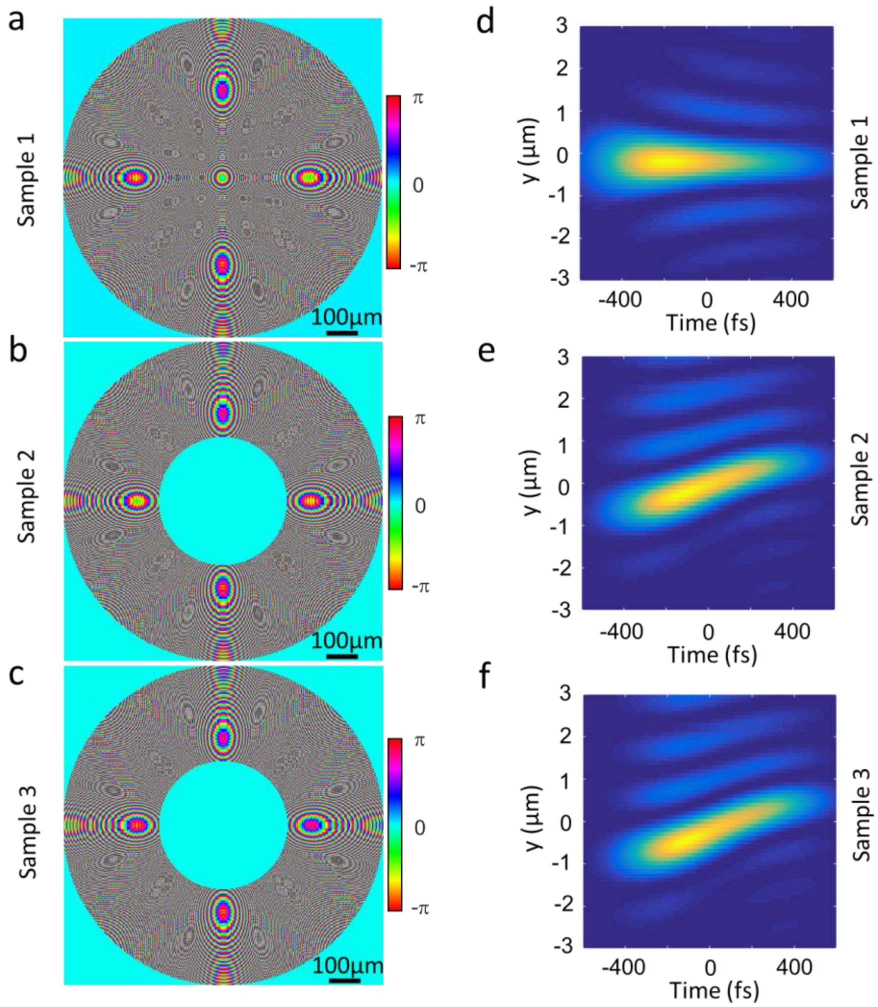


**Extended Data Figure 5. Optical properties of the dispersion-controlled metalenses. (a-c)** Phase profiles encoded in three metalenses (samples 1, 2 and 3) used in this work. **(d-f)** Time-dependent intensity profiles at the focal plane of the metalenses.

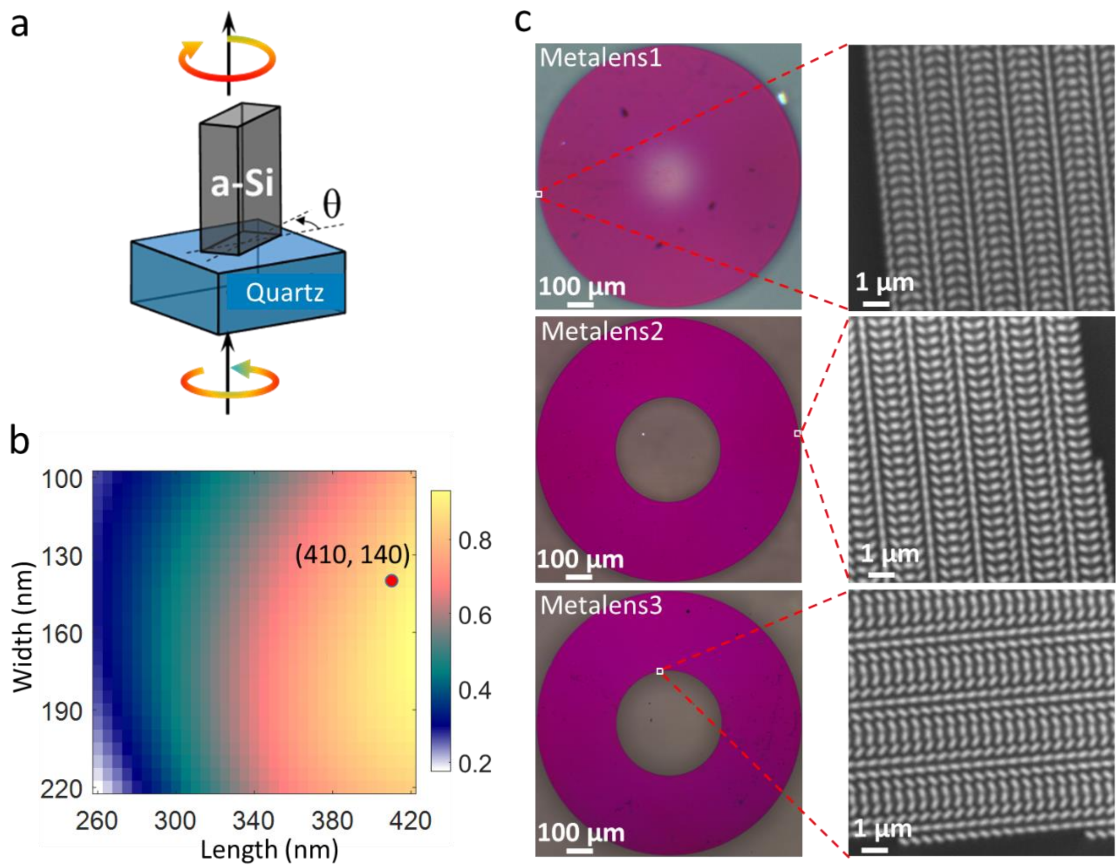


**Extended Data Figure 6. Nanostructures in these dispersion-controlled metalenses. (a)** Sketch for the silicon nanobricks in the metalenses. The amorphous silicon film with a thickness of 760 nm is located on a sapphire substrate. Such a Si-nanobrick can work as a miniaturized half-waveplate, which can change the incident circular polarization into its cross one with an additional phase modulation of twice the rotation angle $\theta$. **(b)** Simulated efficiency of polarization conversion with a function of nanobrick geometry (*i.e.*, width and length). In this work, the 140 nm-width and 410 nm-length geometry of the nanobrick is used after the balance between efficiency and fabrication difficulty. **(c)** Microscopy images of these three metalenses. The images at the left panel are taken by using a 20X objective, while those at the right panel are taken by using an 150X objective lens for a better imaging resolution.

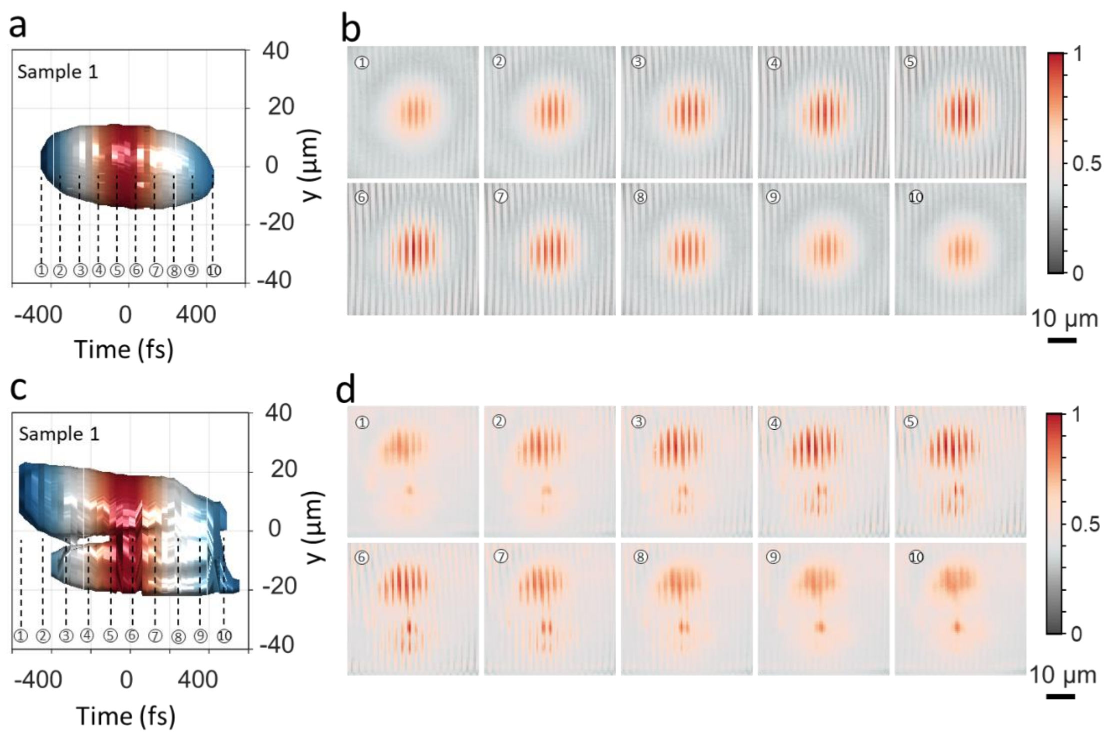


**Extended Data Figure 7. Experimental results for the incident pulse generated by the metalens 1 (sample 1) and its differentiated pulse. (a)** Retrieved iso-intensity profiles of incident pulses generated by sample 1. It is the same with Fig. 3b in main text. **(b)** Measured interference patterns with the temporal indices labelled in **(a)**. **(c)** Retrieved iso-intensity profiles of differentiated pulses by our meta-grating. **(d)** Measured interference patterns with the temporal indices labelled in **(c)**.

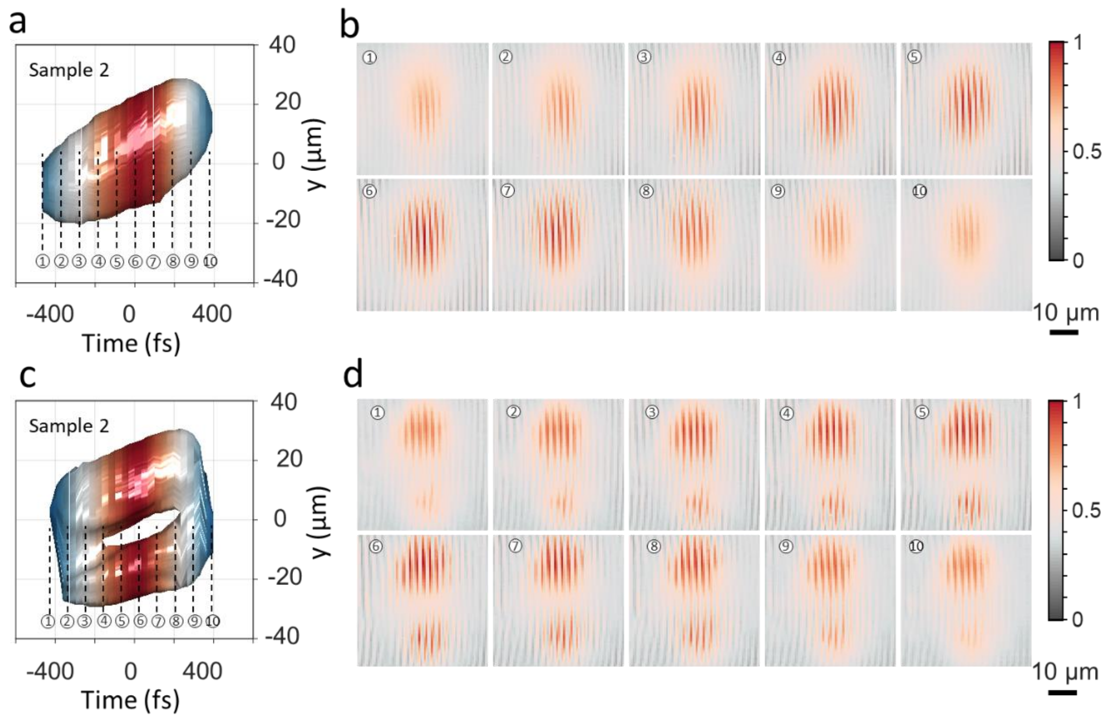


**Extended Data Figure 8. Experimental results for the incident pulse generated by the metalens 2 (sample 2) and its differentiated pulse. (a)** Retrieved iso-intensity profiles of incident pulses generated by sample 2. It is the same with Fig. 3c in main text. **(b)** Measured interference patterns with the temporal indices labelled in **(a)**. **(c)** Retrieved iso-intensity profiles of differentiated pulses by our meta-grating. **(d)** Measured interference patterns with the temporal indices labelled in **(c)**.

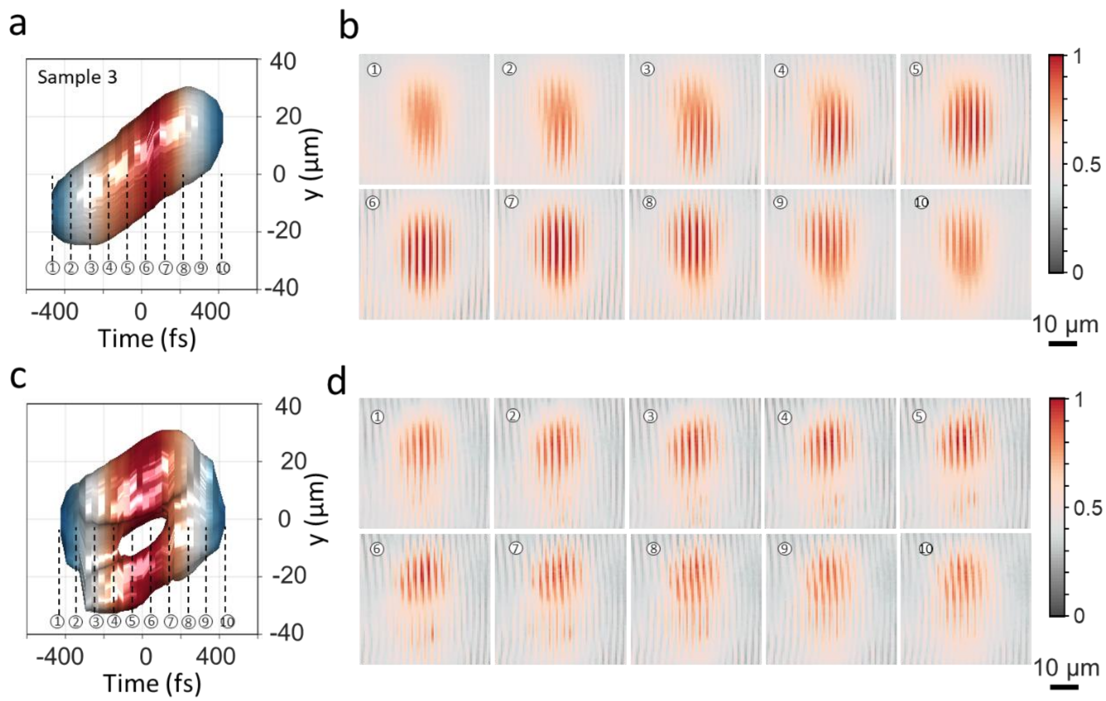


**Extended Data Figure 9. Experimental results for the incident pulse generated by the metalens 3 (sample 3) and its differentiated pulse. (a)** Retrieved iso-intensity profiles of incident pulses generated by sample 3. It is the same with Fig. 3d in main text. **(b)** Measured interference patterns with the temporal indices labelled in **(a)**. **(c)** Retrieved iso-intensity profiles of differentiated pulses by our meta-grating. **(d)** Measured interference patterns with the temporal indices labelled in **(c)**.